# Structural Motifs in Dinuclear $d^8$ Metal Complexes. Structural and Spectroscopic Characteristics of an Alternative Unsymmetrical 3:5 Ligand Distribution As Compared to the Symmetrical 4:4 or Face-to-Face Arrangement

**Alan L. Balch* and Vincent J. Catalano**

Department of Chemistry, University of California, Davis, California 95616

*Received December 12, 1991*

Addition of $[Rh(CNCH_3)_4](BPh_4)$ to an acetone solution of $[Pt(dmp)_2]Cl_2$ (dpm is bis(diphenylphosphino)methane) followed by addition of methanolic ammonium hexafluorophosphate yields ivory $[(CH_3NC)PtRh(CNCH_3)_3(\mu\text{-dpm})_2](PF_6)_3$. Crystals of $[(CH_3NC)PtRh(CNCH_3)_3(\mu\text{-dpm})_2](PF_6)_3 \cdot 0.46(CH_3CH_2)_2O \cdot 0.54CH_3CN$ form in the monoclinic space group $P2_1/n$ (No. 14) with $a = 15.724$ (6) Å, $b = 18.157$ (5) Å, $c = 25.13$ (3) Å, and $\beta = 97.52$ (5)° at 130 K with $Z = 4$. Refinement of 492 parameters and 7788 reflections gave $R = 7.3\%$ and $R_w = 7.6\%$. The cation contains a three-coordinate Pt(II) center datively bonded to a five-coordinate Rh(I) center at a distance of 2.708 (2) Å. Similarly, addition of $Rh(CO)Cl(AsPh_3)_2$ and 3 equiv of methyl isocyanide to $[Pt(dpm)_2]^+$ followed by addition of ammonium hexafluorophosphate leads to formation of yellow $[(CH_3NC)PtRhCl(CNCH_3)_2(\mu\text{-dpm})_2](PF_6)_2$. Yellow crystals of $[(CH_3NC)PtRhCl(CNCH_3)_2(\mu\text{-dpm})_2](PF_6)_2 \cdot 0.5CH_3CN$ form in the triclinic space group $P\bar{1}$ (No. 2) with $a = 11.465$ (4) Å, $b = 14.832$ (6) Å, $c = 19.712$ (10) Å, $\alpha = 87.71$ (4)°, $\beta = 79.43$ (4)°, and $\gamma = 67.98$ (3)° with $Z = 2$ at 130 K. Refinement of 473 parameters and 6461 reflections gave $R = 4.1\%$ and $R_w = 4.2\%$. This complex is structurally similar to $[(CH_3NC)PtRh(CNCH_3)_3(\mu\text{-dpm})_2]^{3+}$, except a chloride is residing in the axial position on the rhodium in place of a methyl isocyanide. Addition of $I_2$ to solutions of $[(CH_3NC)PtRh(CNCH_3)_3(\mu\text{-dpm})_2](PF_6)_3$ does not lead to oxidative addition across the metals but to direct attack on a coordinated methyl isocyanide to produce $[(CH_3NC)PtRhI(CNCH_3)_2(\mu\text{-dpm})_2](PF_6)_2$. Yellow crystals of $[(CH_3NC)PtRhI(CNCH_3)_2(\mu\text{-dpm})_2](PF_6)_2 \cdot CH_3CN$ are essentially isostructural with $[(CH_3NC)PtRhCl(CNCH_3)_2(\mu\text{-dpm})_2](PF_6)_2$ and crystallize in the triclinic space group $P\bar{1}$ (No. 2) with $a = 11.531$ (5) Å, $b = 14.682$ (6) Å, $c = 19.849$ (14) Å, $\alpha = 86.21$ (5)°, $\beta = 78.26$ (5)°, and $\gamma = 68.77$ (3)° with $Z = 2$ at 130 K. Refinement of 438 parameters and 6057 reflections gave $R = 4.2\%$ and $R_w = 4.4\%$. The optical properties of the above three compounds show broad absorbances in the UV region and no photoluminescence. On the basis of their coordination geometry, these three structures are categorized as 3:5 complexes and are contrasted to the well-studied, face-to-face 4:4 complexes. The 4:4 complex, $[(NC)PtRh(CNBu^t)_2(\mu\text{-dpm})_2](PF_6)$ is made by addition of 2 equiv of sodium cyanide to $[Pt(dpm)_2]Cl_2$ followed by addition of $[Rh(CNBu^t)_4](PF_6)$ and ammonium hexafluorophosphate. Red crystals of $[(NC)_2PtRh(CNBu^t)_2(\mu\text{-dpm})_2](PF_6) \cdot 0.5CH_3OH \cdot 0.5(CH_3CH_2)_2O$ crystallize in the orthorhombic space group *Pnma* (No. 62) with $a = 35.723$ (11) Å, $b = 15.214$ (7) Å, and $c = 12.542$ (5) Å with $Z = 4$ at 130 K. Refinement of 244 parameters and 3082 reflections gave $R = 6.5\%$ and $R_w = 6.5\%$. The cation contains a square planar $RhP_2(CNR)_2$ unit and a square planar $PtP_2(CN)_2$ unit connected through the two dpm bridges at a separation of 3.079 (2) Å. The complex in dichloromethane shows a strong absorbance at 470 nm ($\epsilon = 12\,300$ $M^{-1}$ $cm^{-1}$) and photoemissions at 530 nm (fluorescence) and 645 nm (phosphorescence).

## Introduction

Novel features in the absorption and photoemission spectra of dinuclear dimers consisting of two planar four-coordinate $d^8$ metal centers arranged in a face-to-face fashion have made these complexes attractive targets for synthetic and physical studies.[1–7] Extensive work has characterized a range of complexes that include bridged examples such as $[Pt_2(P_2O_5H_2)_4]^{4-}$ [8,9] and $Ir_2(\mu\text{-pz})_2(COD)_2$[10,11] (pz is pyrazolyl; COD is 1,5-cyclooctadiene) as well as unbridged compounds like $[Rh_2(CNR)_8]^{2+}$.[1,12] The ligand arrangement in these symmetrical face-to-face complexes is shown as structure A. We will refer to complexes with this arrangement of ligands as 4:4 complexes.

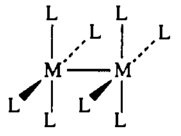

A, 4:4

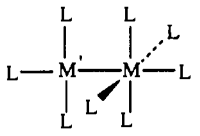

B, 3:5

The purpose of this article is to point out the importance of a second, isomeric ligand arrangement. This is the 3:5 type of complex whose structure is shown as B. In this situation the two metal centers have distinctly different coordination. One is six-coordinate, while the while the other is only four-coordinate with a single donor/acceptor bond connecting the two metal centers. Complexes of 3:5 type have received relatively little attention in comparison to their 4:4 counterparts. Largely, this is due to the current relative rarity of compounds possessing the 3:5 structure.

---

(1) Mann, K. R.; Gordon, J. G., II; Gray, H. B. *J. Am. Chem. Soc.* **1975**, *97*, 3553.
(2) Balch, A. L. *J. Am. Chem. Soc.* **1976**, *98*, 8049.
(3) Balch, A. L.; Tulyathan, B. *Inorg. Chem.* **1977**, *16*, 2840.
(4) Fordyce, W. A.; Brummer, J. G.; Crosby, G. A. *J. Am. Chem. Soc.* **1981**, *103*, 7061.
(5) Fordyce, W. A.; Crosby, G. A. *J. Am. Chem. Soc.* **1982**, *104*, 985.
(6) Stein, P.; Dickson, M. K.; Roundhill, D. M. *J. Am. Chem. Soc.* **1983**, *105*, 3489.
(7) Smith, D. C.; Gray, H. B. *Coord. Chem. Rev.* **1990**, *100*, 160.
(8) Roundhill, D. M.; Gray, H. B.; Che, C.-M. *Acc. Chem. Res.* **1989**, *22*, 55.
(9) Zipp, A. P. *Coord. Chem. Rev.* **1988**, *84*, 47.
(10) Marshall, J. L.; Stobart, S. R.; Gray, H. B. *J. Am. Chem. Soc.* **1984**, *106*, 3027.
(11) Caspar, J. V.; Gray, H. B. *J. Am. Chem. Soc.* **1984**, *106*, 3029.
(12) Mann, K. R.; Lewis, N. S.; Williams, R. M.; Gray, H. B.; Gordon, J. G., II. *Inorg. Chem.* **1978**, *17*, 828.

0020-1669/92/1331-3934$03.00/0

**Table I.** NMR Spectral Data

| | $^{31}$P NMR$^a$ | | | | | $^1$H NMR | |
|---|---|---|---|---|---|---|---|
| compd | δ, ppm$^b$ | $^1J$(Pt,P), Hz | δ, ppm$^c$ | $^1J$(Rh,P), Hz | $^{195}$Pt NMR δ, ppm | $J$(Pt,H) for δ(CH$_2$), Hz | δ(CNR), ppm |
| **1** | 0.3 | 2374.7 | 13.4 | 80 | –4534 | 5.10 | 2.61 |
| **2** | 11.7 | 2443.1 | 13.4 | 67 | –4536 | 5.19 | 2.87,$^d$ 2.26$^e$ |
| **3** | 12.2 | 2138 | 7.5 | 69 | | 5.3 | 2.82,$^d$ 2.25$^e$ |
| **4** | 1.7 | 2482.7 | 18.4 | 124.2 | –4485 | 5.48 | 0.81 |

$^a$ Recorded in acetonitrile solution at 23 °C. $^b$ Pt-bound phosphorus. $^c$ Rh-bound phosphorus. $^d$ Rh-bound isocyanide (intensity 6). $^e$ Pt-bound isocyanide (intensity 3).

**Scheme I**

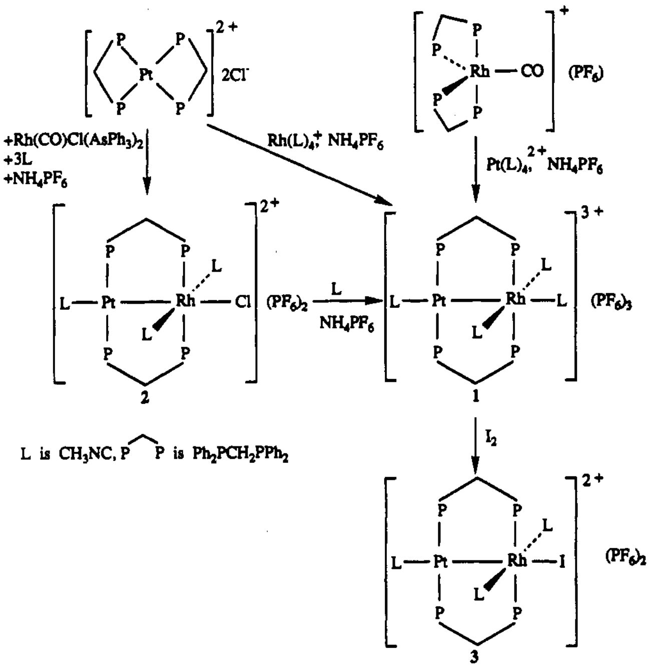

However, some do exist,[13] and one case of a pair of isomers, one with a 4:4 structure, the other with a 3:5 structure, is known.[14] Here we present data regarding the synthesis, structure, and spectroscopic characterization of three complexes with the 3:5 structure and compare those to a closely related substance with a 4:4 geometry. In a previous article we described the preparation and structure of a second, independent group of compounds with the 3:5 structure.[15]

## Results

**Synthetic Studies.** Reactions that lead to the formation of a family of 3:5 complexes are set out in Scheme I. Treatment of Pt(dpm)$_2^{2+}$ with Rh(CNMe)$_4^+$ in the presence of ammonium hexafluorophosphate yields ivory [(MeNC)PtRh(CNMe)$_3$(μ-dpm)$_2$](PF$_6$)$_3$ (**1**). The same complex is obtained when the locations of the ligands on the starting complexes are reversed. Thus, addition of Pt(CNMe)$_4^{2+}$ to Rh(CO)(dpm)$_2^+$ also produces **1**. The reaction of Rh(CO)Cl(AsPh$_3$)$_2$ with Pt(dpm)$_2^{2+}$ in the presence of 3 equiv of methyl isocyanide and ammonium hexafluorophosphate forms yellow [(MeNC)PtRhCl(CNMe)$_2$(μ-dpm)$_2$](PF$_6$)$_2$ (**2**), which can be converted to **1** by the addition of more methyl isocyanide. In exploring these routes to **1**, we have carefully looked for the formation of an isomeric form that might have the 4:4 structure. However, no evidence for the formation of any isomeric form has been found, and it appears that **1** is the thermodynamically most stable form of this dinuclear compound. Compound **1** is soluble in acetonitrile and nitromethane, moderately soluble in acetone, and slightly soluble in dichloromethane, while **2** is soluble in acetonitrile, acetone, and dichloromethane and slightly soluble in chloroform. Both **1** and **2** are insoluble in methanol, ethyl ether, and hydrocarbons.

Oxidative addition of halogens to 4:4 complexes are known to strengthen the metal–metal bonding within the dinuclear unit. However, when diiodine is added to **1** followed by the addition of ammonium hexafluorophosphate in methanol, the result is the formation of [(MeNC)PtRhI(CNMe)$_2$(μ-dpm)$_2$](PF$_6$)$_2$ (**3**) a product of apparent substitution of iodide for an isocyanide ligand. Surprisingly, addition of iodide (as sodium iodide) to **1** does not result in the formation of **3**. Another, unidentified product is formed. The reaction of diiodine with **1** is probably initiated by attack of diiodine on the coordinated isocyanide with the eventual loss of MeN=C(Cl)I.

In marked contrast, the reaction of [Pt(dpm)$_2$]Cl$_2$ with sodium cyanide and [Rh(CNBu$^t$)$_4$]$^+$ in the presence of ammonium hexafluorophosphate yields the 4:4 compound [(NC)$_2$PtRh(CNBu$^t$)$_2$(μ-dpm)$_2$](PF$_6$) (**4**; eq 1). The use of *tert*-butyl isocyanide is not critical to the reactivity; a similar reaction occurs with [Rh(CNMe)$_4$]$^+$. However, in the latter case, there is severe disorder of the cation in the crystalline product, and characterization of the solid-state structure was hampered. With the greater size of the *tert*-butyl group, the two ends of the cation of **4** are sufficiently different so that disorder does not occur in the crystalline state.

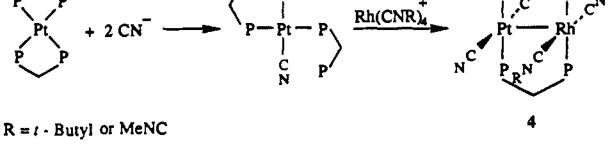

(1)

R = *t* - Butyl or MeNC

Infrared spectral parameters for these complexes are given in the Experimental Section. All complexes, **1**–**4**, show only terminal isocyanide stretching vibrations in their infrared spectra. NMR spectral data are collected in Table I. The $^{31}$P{$^1$H} NMR spectra of **1** and **4** consist of an apparent triplet with satellites for the two phosphorus atoms bound to platinum and a doublet of apparent triplets for the phosphorus atoms bound to rhodium. The $^{31}$P{$^1$H} NMR spectra of **2** and **3** are related, but the proximity of chemical shifts for the two different phosphorus environments increase the spectral complexity due to second-order effects. The complex P–P coupling has not been amenable to thorough analysis because of spectral resolution. The variation in $^1J$(Pt,P) is small within this group of complexes, but $^1J$(Rh,P) is much greater for **4** than for **1**–**3**. The $^{195}$Pt spectra consist of a single triplet for all four complexes. The value of $J$(Pt,Rh) must be less than the line width (ca. 100 Hz). The $^1$H NMR spectra show a multiplet at ca 5.1 ppm for the methylene protons of the bridging diphosphine with satellites due to coupling to $^{195}$Pt and a broad signal for the bound isocyanide ligands. In complex **1**, the individual isocyanide environments are not distinguished. This may be due to insufficient resolution or to fluxional effects.

**Structures of the 3:5 Complexes, [(MeNC)PtRh(CNMe)$_3$(μ-dpm)$_2$](PF$_6$)$_3$, [(MeNC)PtRhCl(CNMe)$_2$(μ-dpm)$_2$](PF$_6$)$_2$, and [(MeNC)PtRhI(CNMe)$_2$(μ-dpm)$_2$](PF$_6$)$_2$.** The asymmetric unit

---

(13) Farr, J. P.; Olmstead, M. M.; Balch, A. L. *J. Am. Chem. Soc.* **1980**, *102*, 6654.

(14) Balch, A. L.; Guimerans, R. R.; Linehan, J.; Olmstead, M. M.; Oram, D. E. *Organometallics* **1985**, *4*, 1445.

(15) Balch, A. L.; Catalano, V. J. *Inorg. Chem.* **1992**, *31*, 2569.

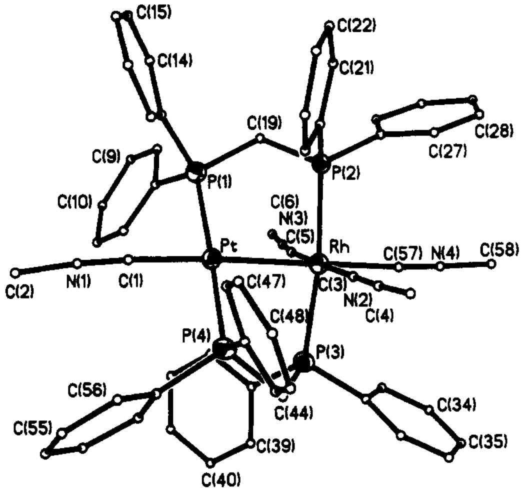

**Figure 1.** Perspective view of the cation in $[(MeNC)PtRh(CNMe)_3(\mu\text{-dpm})_2](PF_6)_3$ with 50% thermal contours for heavy atoms and uniform, arbitrarily sized circles for carbon and nitrogen atoms.

**Table II.** Selected Interatomic Distances and Angles in 3:5 Complexes $[(CH_3NC)PtRh(CNCH_3)_3(\mu\text{-dpm})_2]^{3+}$ (**1**), $[(CH_3NC)PtRhCl(CNCH_3)_2(\mu\text{-dpm})_2]^{2+}$ (**2**), and $[(CH_3NC)PtRhI(CNCH_3)_2(\mu\text{-dpm})_2]^{2+}$ (**3**)

| | **1** | **2** | **3** |
|---|---|---|---|
| | Distances (Å) | | |
| Pt–Rh | 2.708 (2) | 2.688 (2) | 2.703 (2) |
| Pt–P(1) | 2.316 (4) | 2.310 (2) | 2.309 (3) |
| Pt–P(4) | 2.311 (4) | 2.300 (2) | 2.299 (3) |
| Pt–C(1) | 1.97 (1) | 1.960 (10) | 1.963 (10) |
| Rh–P(2) | 2.344 (4) | 2.336 (4) | 2.361 (3) |
| Rh–P(3) | 2.334 (4) | 2.342 (2) | 2.357 (3) |
| Rh–C(3) | 1.95 (1) | 1.976 (9) | 1.955 (8) |
| Rh–C(5) | 1.97 (2) | 1.961 (9) | 1.982 (9) |
| Rh–X | 2.06 (1) | 2.516 (3) | 2.807 (2) |
| | Angles (deg) | | |
| Rh–Pt–C(1) | 175.9 (4) | 166.4 (3) | 167.5 (3) |
| Rh–Pt–P(1) | 91.3 (1) | 90.5 (1) | 91.0 (1) |
| Rh–Pt–P(4) | 91.0 (1) | 91.7 (1) | 91.5 (1) |
| P(1)–Pt–P(4) | 177.6 (1) | 169.0 (1) | 169.2 (1) |
| P(1)–Pt–C(1) | 90.0 (4) | 92.6 (2) | 92.2 (2) |
| P(4)–Pt–C(1) | 87.7 (4) | 87.7 (2) | 87.6 (2) |
| Pt–Rh–X | 178.4 (4) | 173.1 (1) | 175.0 (1) |
| Pt–Rh–P(2) | 86.1 (1) | 94.1 (1) | 93.7 (1) |
| Pt–Rh–P(3) | 86.4 (1) | 95.2 (1) | 95.1 (1) |
| Pt–Rh–C(3) | 89.2 (4) | 81.4 (3) | 80.9 (3) |
| Pt–Rh–C(5) | 93.6 (4) | 89.5 (3) | 88.2 (3) |
| P(2)–Rh–P(3) | 172.3 (1) | 170.7 (1) | 171.2 (1) |
| P(2)–Rh–C(3) | 92.5 (4) | 90.7 (2) | 89.6 (2) |
| P(2)–Rh–C(5) | 87.4 (5) | 93.4 (2) | 93.6 (2) |
| P(2)–Rh–X | 93.3 (4) | 82.8 (1) | 84.1 (2) |
| P(3)–Rh–C(3) | 89.0 (4) | 91.4 (2) | 91.7 (2) |
| P(3)–Rh–C(5) | 91.5 (5) | 86.0 (2) | 86.8 (2) |
| P(3)–Rh–X | 94.2 (4) | 88.1 (1) | 87.1 (1) |
| C(3)–Rh–C(5) | 176.7 (5) | 170.3 (4) | 168.8 (4) |
| C(3)–Rh–X | 89.4 (5) | 92.4 (3) | 94.5 (3) |
| C(5)–Rh–X | 87.4 (5) | 96.8 (3) | 96.5 (3) |
| Pt–C(1)–N(1) | 175 (1) | 169.4 (8) | 167.6 (10) |
| Rh–C(3)–N(2) | 175 (1) | 176.2 (7) | 176.9 (10) |
| Rh–C(5)–N(3) | 173 (1) | 176.8 (7) | 176.5 (10) |
| Rh–C(57)–N(4) | 176 (1) | | |
| P(1)–C(19)–P(2) | 107.1 (6) | 111.5 (4) | 112.4 (4) |
| P(3)–C(44)–P(4) | 108.1 (7) | 111.5 (4) | 110.3 (4) |

**Table III.** Selected Atomic Coordinates (×10⁴) and Equivalent Isotropic Displacement Coefficients ($Å^2 \times 10^3$) for $[(MeNC)PtRh(CNMe)_3(\mu\text{-dpm})_2](PF_6)_3\cdot 0.46Et_2O\cdot 0.54MeCN^a$

| | *x* | *y* | *z* | *U*(eq)[b] |
|---|---|---|---|---|
| Pt | 8945 (1) | 2288 (1) | 1826 (1) | 20 (1)* |
| Rh | 10266 (1) | 3091 (1) | 2325 (1) | 20 (1)* |
| P(1) | 9620 (2) | 1199 (2) | 2115 (1) | 22 (1)* |
| P(2) | 11150 (2) | 2131 (2) | 2102 (1) | 19 (1)* |
| P(3) | 9232 (2) | 3941 (2) | 2514 (1) | 22 (1)* |
| P(4) | 8237 (2) | 3347 (2) | 1508 (1) | 24 (1)* |
| N(1) | 7309 (7) | 1424 (7) | 1339 (5) | 35 (4) |
| N(2) | 10420 (7) | 3946 (6) | 1276 (5) | 26 (4) |
| N(3) | 10325 (8) | 2345 (8) | 3441 (5) | 41 (5) |
| N(4) | 11863 (7) | 4019 (7) | 2899 (5) | 33 (4) |
| C(1) | 7937 (9) | 1729 (8) | 1502 (6) | 27 (3) |
| C(2) | 6520 (10) | 1086 (9) | 1160 (7) | 48 (4) |
| C(3) | 10340 (8) | 3606 (7) | 1652 (5) | 23 (3) |
| C(4) | 10530 (10) | 4319 (9) | 782 (6) | 40 (4) |
| C(5) | 10249 (9) | 2601 (7) | 3024 (6) | 28 (3) |
| C(6) | 10450 (14) | 2034 (11) | 3977 (8) | 73 (6) |
| C(8) | 9591 (10) | 328 (9) | 3022 (6) | 42 (4) |
| C(9) | 9238 (11) | 57 (10) | 3461 (7) | 49 (4) |
| C(10) | 8438 (10) | 299 (8) | 3553 (8) | 38 (4) |
| C(11) | 7972 (10) | 772 (9) | 3211 (6) | 40 (4) |
| C(57) | 11284 (8) | 3708 (7) | 2685 (5) | 23 (3) |
| C(58) | 12638 (7) | 4380 (6) | 3165 (5) | 51 (5) |

[a] Parameters for dpm carbon atoms, hexafluorophosphate anions, diethyl ether, and acetonitrile omitted. See supplementary material. [b] An asterisk indicates the equivalent isotropic *U* defined as one third-of the trace of the orthogonalized $U_{ij}$ tensor.

for $[(MeNC)PtRh(CNMe)_3(\mu\text{-dpm})_2](PF_6)_3\cdot 0.46(C_2H_5)_2O\cdot 0.54CH_3CN$ consists of the cation, one ordered and two disordered hexafluorophosphate anions, and 0.46 ethyl ether and 0.54 acetonitrile solvate. There are no unusual contacts between these subunits. Figure 1 shows a drawing of the cation. Table II contains selected interatomic distances and angles. Table III contains selected atomic coordinates.

The cation has a 3:5 structure with a pair of trans bridging dpm ligands that connect rhodium and platinum. The distribution of methyl isocyanide ligands is uneven with three on rhodium and one on platinum. The Pt–Rh distance of 2.709 (2) Å is consistent with the presence of a single bond between these atoms. Other distances within the cation fall within normal limits. The Rh–C(57) distance (2.07 (1) Å) that involves the ligand trans to the Pt–Rh bond is marginally longer than the other two Rh–C distances (1.96 (1) and 1.96 (2) Å), but the Pt–C(1) distance (1.96 (1) Å) is the same.

The cis bond angles about both rhodium and platinum cluster about 90° as expected. The ligand arrangement on rhodium is staggered with respect to the P(1)–Pt–P(4) unit. Thus, the P(1)–Pt–Rh–P(2) and P(4)–Pt–Rh–P(3) dihedral angles are 37.6 and 40.0°, respectively.

The structure of the cation in $[(MeNC)PtRhCl(CNMe)_2(\mu\text{-dpm})_2](PF_6)_2\cdot 0.5CH_3CN$ is similar to that in **1**. The asymmetric unit for this salt consists of the cation, two hexafluorophosphate anions, and a site which is half-occupied by a molecule of acetonitrile. A view of the cation is shown in Figure 2. Interatomic distances and angles are presented in Table II. Selected atomic coordinates are given in Table IV. In the solid state, $[(MeNC)PtRhI(CNMe)_2(\mu\text{-dpm})_2](PF_6)_2\cdot 0.5CH_3CN$ is essentially isostructural with its chloride analog. Interatomic distances and angles are given in Table II, and atomic coordinates are in Table V.

The cations in **2** and **3** belong to the 3:5 structural type. Each platinum is four-coordinate with bonds to a single terminal isocyanide, to two trans phosphines, and to the rhodium. The rhodium ions are six-coordinate with bonds to two trans isocyanides, to two trans phosphines, to the terminal halide (chloride or iodide), and to platinum. The Pt–Rh distances in **2** and **3** (2.688 (2) and 2.703 (2) Å) are virtually identical to that of **1**. Other bond distances are, in general, similar within the group **1**–**3**. One major difference of course is the rhodium ligand trans to the Pt–Rh bond, which is Cl in **2** and I in **3**. The Rh–Cl bond in **2** is unusually long. Typical terminal Rh–Cl bonds lengths fall in the range 2.3–2.4 Å.[16,17] The elongation seen for **2** is due to the trans effect

---

[16] Balch, A. L.; Ghedini, M.; Oram, D. E.; Reedy, P. E., Jr. *Inorg. Chem.* **1987**, *26*, 1223.

[17] Farr, J. P.; Olmstead, M. M.; Balch, A. L. *Inorg. Chem.* **1983**, *22*, 1229.

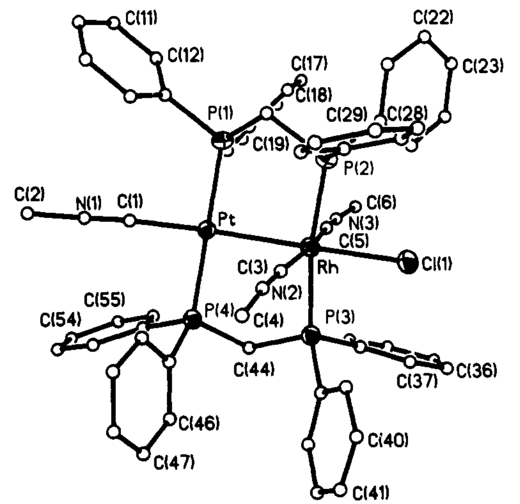

**Figure 2.** Perspective view of the cation in [(MeNC)PtRhCl(CNMe)$_2$($\mu$-dpm)$_2$](PF$_6$)$_2$ plotted as described for Figure 1. The structure for [(MeNC)PtRhI(CNMe)$_2$($\mu$-dpm)$_2$](PF$_6$)$_2$ is similar with iodide in place of chloride.

**Table IV.** Selected Atomic Coordinates ($\times 10^4$) and Equivalent Isotropic Displacement Coefficients (Å$^2$ × 10$^3$) for [(MeNC)PtRhCl(CNMe)$_2$($\mu$-dpm)$_2$](PF$_6$)$_2$·0.5CH$_3$CN[a]

| | *x* | *y* | *z* | *U*(eq)[b] |
|---|---|---|---|---|
| Rh | 3267 (1) | 3039 (1) | 2400 (1) | 22 (1)* |
| Pt | 1904 (1) | 1888 (1) | 2607 (1) | 20 (1)* |
| N(1) | 808 (7) | 366 (5) | 3198 (3) | 35 (3) |
| N(2) | 4655 (7) | 1730 (5) | 3514 (4) | 32 (3) |
| N(3) | 1858 (7) | 4033 (5) | 1207 (4) | 31 (3) |
| N(4) | 3043 (15) | 7489 (13) | 3497 (9) | 73 (6) |
| Cl(1) | 4582 (2) | 4077 (2) | 2354 (1) | 35 (1)* |
| P(1) | 85 (2) | 3200 (2) | 3057 (1) | 24 (1)* |
| P(2) | 1860 (2) | 4216 (2) | 3242 (1) | 26 (1)* |
| P(3) | 4840 (2) | 2042 (2) | 1523 (1) | 23 (1)* |
| P(4) | 3545 (2) | 627 (2) | 1972 (1) | 22 (1)* |
| C(1) | 1118 (8) | 949 (6) | 2944 (4) | 25 (2) |
| C(2) | 407 (11) | −355 (8) | 3550 (6) | 74 (4) |
| C(3) | 4106 (8) | 2221 (6) | 3120 (5) | 28 (4) |
| C(4) | 5416 (10) | 1108 (7) | 3971 (5) | 52 (5) |
| C(5) | 2344 (8) | 3670 (6) | 1659 (4) | 24 (3) |
| C(6) | 1288 (10) | 4616 (6) | 662 (5) | 45 (4) |

[a] Carbon atoms of dpm and parameters for hexafluorophosphate and acetonitrile omitted. See supplementary material. [b] An asterisk indicates the equivalent isotropic *U* defined as one-third of the trace of the orthogonalized U$_{ij}$ tensor.

of the Pt–Rh bond. Interestingly, there is no comparable lengthening of the Pt–C bond in **1**–**3**. The Rh–I bond length in **3** is typical for situations where the Rh–I bond is trans to a rhodium–metal bond.[18]

Bond angles within **2** and **3** are very similar and are in general quite like those in **1**. However, **2** and **3** are less twisted than **1** in the orientation of the P–Rh–P and P–Pt–P units. Thus, the P(1)–Pt–Rh–P(2) and P(4)–Pt–Rh–P(3) dihedral angles in **2** are 23.2 and 13.2° and in **3** are 23.2 and 12.6°.

**Structure of the 4:4 Complex, [(NC)$_2$PtRh(CNBu$^t$)$_2$($\mu$-dpm)$_2$](PF$_6$)·0.5(C$_2$H$_5$)$_2$O·0.5CH$_3$OH.** The asymmetric unit contains half of a complex cation, half of a hexafluorophosphate anion, one-quarter of a molecule of ethyl ether, and one-quarter of a methanol molecule. These components are well separated from one another.

Figure 3 shows a drawing of the cation which belongs to the 4:4 structural type. Selected interatomic distances and angles are in Table VI. A selection of atomic coordinates is given in Table VII. A crystallographic mirror plane passes through the platinum, rhodium, and the *tert*-butyl isocyanide and cyanide ligands of the cation. Each metal ion is four-coordinate. The platinum is coordinated by the trans phosphine ligands and trans, terminal cyanide ligands. The rhodium is bonded to trans, terminal *tert*-butyl isocyanide ligands and the trans phosphine ligands. Because of the mirror symmetry the coordination planes of the two metal ions are fully eclipsed. The Pt–Rh distance is 3.079 (2) Å, a distance that is typical of 4:4 or face-to-face di-

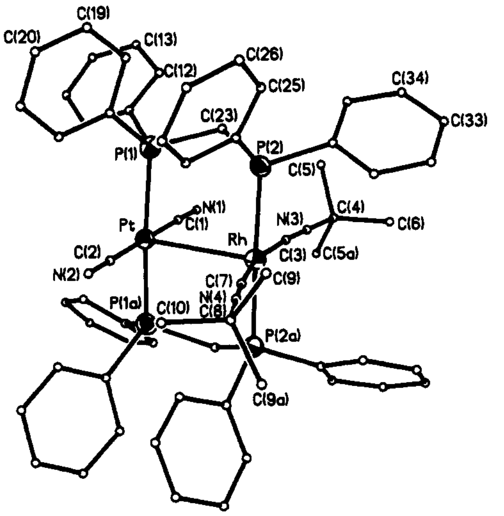

**Figure 3.** Perspective drawing of the cation in [(NC)$_2$PtRh(CNBu$^t$)$_2$($\mu$-dpm)$_2$](PF$_6$) plotted as described for Figure 1.

**Table V.** Selected Atomic Coordinates ($\times 10^4$) and Equivalent Isotropic Displacement Coefficients (Å$^2$ × 10$^3$) for [(MeNC)PtRhI(CNMe)$_2$($\mu$-dpm)$_2$](PF$_6$)$_2$·CH$_3$CN[a]

| | *x* | *y* | *z* | *U*(eq)[b] |
|---|---|---|---|---|
| Pt | 2024 (1) | 6884 (1) | 2594 (1) | 15 (1)* |
| Rh | 3393 (1) | 8067 (1) | 2369 (1) | 17 (1)* |
| I(1) | 4850 (1) | 9262 (1) | 2255 (1) | 30 (1)* |
| P(1) | 214 (3) | 8176 (1) | 3036 (1) | 18 (1)* |
| P(2) | 1978 (3) | 9227 (1) | 3205 (1) | 21 (1)* |
| P(3) | 4987 (3) | 7068 (1) | 1507 (1) | 19 (1)* |
| P(4) | 3660 (3) | 5637 (1) | 1973 (1) | 18 (1)* |
| N(1) | 935 (9) | 5324 (4) | 3177 (3) | 28 (2) |
| N(2) | 4674 (8) | 6786 (4) | 3516 (3) | 23 (2) |
| N(3) | 1993 (8) | 9048 (4) | 1182 (3) | 20 (1) |
| C(1) | 1220 (10) | 5925 (5) | 2927 (4) | 20 (2) |
| C(2) | 537 (12) | 4551 (7) | 3536 (5) | 53 (3) |
| C(3) | 4165 (10) | 7261 (5) | 3098 (4) | 22 (2) |
| C(4) | 5416 (11) | 6172 (6) | 3994 (5) | 41 (3) |
| C(5) | 2465 (10) | 8688 (5) | 1623 (4) | 19 (2) |
| C(6) | 1423 (10) | 9612 (5) | 644 (4) | 29 (2) |

[a] Carbon atoms of dpm and parameters for hexafluorophosphate and acetonitrile omitted. See supplementary material. [b] An asterisk indicates the equivalent isotropic *U* defined as one-third of the trace of the orthogonalized U$_{ij}$ tensor.

**Table VI.** Selected Interatomic Distances and Angles in [(NC)$_2$PtRh(CNBu$^t$)$_2$($\mu$-dpm)$_2$](PF$_6$) (**4**)

| | | | |
|---|---|---|---|
| | Distances (Å) | | |
| Pt–Rh | 3.079 (2) | | |
| Pt–P(1) | 2.334 (4) | Rh–P(2) | 2.300 (4) |
| Pt–C(1) | 2.035 (2) | Rh–C(3) | 1.96 (2) |
| Pt–C(2) | 2.02 (2) | Rh–C(7) | 1.95 (2) |
| | Angles (deg) | | |
| P(1)–Pt–P(1) | 168.2 (2) | P(2)–Rh–P(2) | 173.5 (2) |
| P(1)–Pt–C(1) | 84.1 (1) | P(2)–Rh–C(3) | 86.8 (1) |
| P(1)–Pt–C(2) | 95.9 (1) | P(2)–Rh–C(7) | 93.2 (1) |
| P(1)–Pt–Rh | 91.0 (1) | P(2)–Rh–Pt | 89.3 (1) |
| C(1)–Pt–C(2) | 179.5 (8) | C(3)–Rh–C(7) | 166.1 (8) |
| C(1)–Pt–Rh | 95.3 (6) | C(3)–Rh–Pt | 86.6 (6) |
| C(2)–Pt–Rh | 84.2 (6) | C(7)–Rh–Pt | 107.3 (6) |
| Pt–C(1)–N(1) | 178.0 (2) | Rh–C(3)–N(3) | 174.3 (1) |
| Pt–C(2)–N(2) | 179.6 (11) | Rh–C(7)–N(4) | 176.0 (2) |
| P(1)–C(23)–P(2) | 116.1 (7) | | |

---

[18] Olmstead, M. M.; Guimerans, R. R.; Balch, A. L. *Inorg. Chem.* **1983**, *22*, 2473.

**Table VII.** Selected Atomic Coordinates ($\times 10^4$) and Equivalent Isotropic Displacement Coefficients ($\text{Å}^2 \times 10^3$) for $[(NC)_2PtRh(CNBu^t)_2(\mu\text{-dpm})_2](PF_6)\cdot0.25MeOH\cdot0.25Et_2O$[a]

| | $x$ | $y$ | $z$ | $U$(eq)[b] |
|---|---|---|---|---|
| Pt | 948 (1) | 2500 | 2066 (1) | 22 (1)* |
| Rh | 1667 (1) | 2500 | 3420 (1) | 23 (1)* |
| P(1) | 975 (1) | 4026 (3) | 1891 (3) | 28 (1)* |
| P(2) | 1680 (1) | 4009 (3) | 3323 (3) | 25 (1)* |
| N(1) | 1375 (5) | 2500 | −151 (14) | 39 (7) |
| N(2) | 534 (5) | 2500 | 4300 (14) | 39 (7) |
| N(3) | 2128 (5) | 2500 | 1346 (13) | 31 (6) |
| N(4) | 1446 (5) | 2500 | 5808 (14) | 31 (6) |
| C(1) | 1216 (6) | 2500 | 639 (18) | 28 (5) |
| C(2) | 685 (6) | 2500 | 3491 (17) | 25 (5) |
| C(3) | 1941 (5) | 2500 | 2070 (18) | 26 (5) |
| C(4) | 2376 (7) | 2500 | 427 (19) | 44 (6) |
| C(5) | 2298 (5) | 3316 (12) | −244 (13) | 58 (5) |
| C(6) | 2774 (6) | 2500 | 723 (20) | 69 (9) |
| C(7) | 1515 (5) | 2500 | 4915 (17) | 22 (5) |
| C(8) | 1370 (6) | 2500 | 6966 (17) | 32 (5) |
| C(9) | 1550 (4) | 3327 (10) | 7449 (13) | 50 (4) |
| C(10) | 945 (6) | 2500 | 7097 (19) | 47 (6) |

[a] Carbon atoms of dpm and parameters for hexafluorophosphate, methanol, and ethyl ether omitted. See supplementary material. [b] An asterisk indicates the equivalent isotropic $U$ defined as one-third of the trace of the orthogonalized $U_{ij}$ tensor.

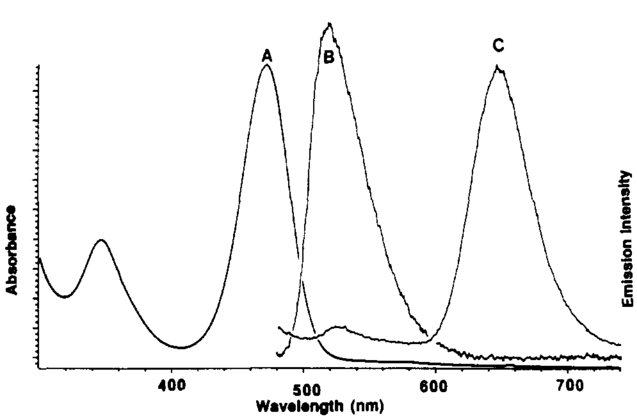

**Figure 4.** Electronic absorption spectrum (A) of a dichloromethane solution of $[(NC)_2PtRh(CNBu^t)_2(\mu\text{-dpm})_2](PF_6)$ at 23 °C. Trace B shows the emission spectrum for the solution at 23 °C with excitation at 470 nm, while trace C shows the emission recorded for the sample frozen at 77 K with excitation at 470 nm.

nuclear complexes (vide infra). Other distances within the cation are unexceptional. Bond angles within the cation are also highly regular.

**Electronic Absorption and Emission Spectra.** The electronic spectral features for the 4:4 complex, **4**, are typical for species of this structural type. Figure 4 shows the relevant data. Trace A shows the absorption spectrum for an acetonitrile solution at 23 °C. It is dominated by a strong absorption at 470 nm with $\epsilon = 12\,300$ M$^{-1}$ cm$^{-1}$. A second strong band seen at 346 nm with $\epsilon = 4700$ M$^{-1}$ cm$^{-1}$. A weak feature at 580 nm ($\epsilon = 900$ M$^{-1}$ cm$^{-1}$) is believed to be the spin-forbidden counterpart of the 470-nm feature. This strong band is assigned as the allowed $\sigma^*(d_{z^2}\ d_{z^2}) \rightarrow \sigma(p_z\ p_z)$ transition. Trace B represents the emission spectrum gathered from acetonitrile solution of **4** with excitation at 470 nm. Strong emission at 530 nm is observed. When the sample is frozen at 77 K, the emission spectrum shown in trace C is observed. At this temperature a strong emission at 645 nm develops and dominates the spectrum, while a weaker feature is also present at 530 nm. Examination of the excitation profile shows that the emission at 645 nm is pumped by both the strong absorption at 470 nm and the much weaker absorption at 580 nm.

Corresponding absorption data for the 3:5 complexes, **1**–**3**, are shown in Figure 5. The spectra lack the intense, proximity shifted band in the visible range that is characteristic of the 4:4 type complexes. Rather a series of poorly resolved features are seen at higher energies. The spectra of **2** and **3** show features at lower energies than **1**. These are probably halide-to-metal charge-transfer absorptions. The fact that these bands appear at lower energies for iodide (for **3**) than for chloride (for **2**) is consistent with that assignment as is the fact that these are absent in **1**. Samples of **1** do not show photoluminescence at 25 °C or when frozen at 77 K.

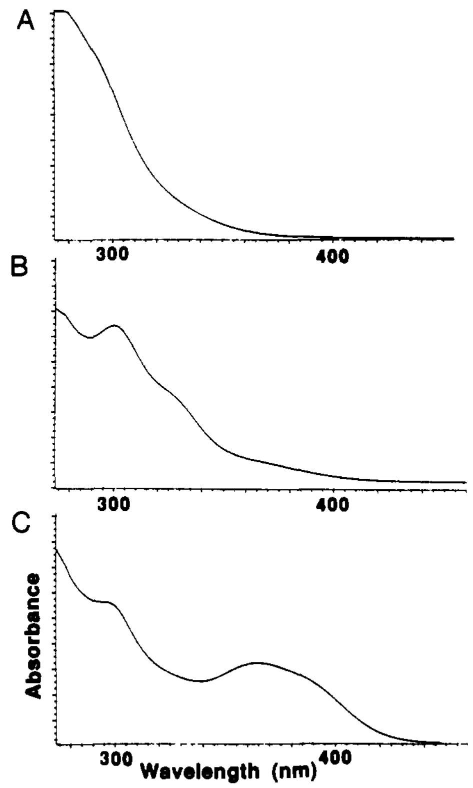

**Figure 5.** Electronic absorption spectra of dichloromethane solutions at 23 °C [$\lambda_{max}$, nm ($\epsilon$, M$^{-1}$ cm$^{-1}$)]: (A, **1**) 289 sh (30 600), 325 (9700), 366 (1500); (B, **2**) 300 (23 600), 326 sh (13 800), 370 sh (3700); (C, **3**) 298 (20 600), 364 (11 900), 390 sh (9000).

## Discussion

The structures, electronic absorption and emission spectra, bonding characteristics, and chemical and photochemical reactivity of dinuclear d$^8$ complexes possessing the 4:4 structural type have received considerable attention. Table VIII presents a

---

(19) Filomena Dos Remedios Pinto, M. A.; Sadler, P. J.; Neidle, S.; Sanderson, M. R.; Subbiah, A. J.; Kuroda, R. *Chem. Soc., Chem. Commun.* **1980**, 13.

(20) Beveridge, K. A.; Bushnell, G. W.; Dixon, K. R.; Eadie, D. T.; Stobart, S. R.; Atwood, J. L.; Zaworotko, M. J. *J. Am. Chem. Soc.* **1982**, *104*, 922.

(21) Cowie, M.; Dwight, S. K. *Inorg. Chem.* **1980**, *19*, 2500.

(22) Kenney, M. I. S.; Kenney, J. W., III; Crosby, G. A. *Organometallics* **1986**, *5*, 230.

(23) Mague, J. T. *Inorg. Chem.* **1969**, *8*, 1975.

(24) Mann, K. R.; Thich, J. A.; Bell, R. A.; Cayle, C. L.; Gray, H. B. *Inorg. Chem.* **1980**, *19*, 2462.

(25) Rodman, G. S.; Mann, K. R. *Inorg. Chem.* **1988**, *27*, 3338.

(26) Rodman, G. S.; Daws, C. A.; Mann, K. R. *Inorg. Chem.* **1988**, *27*, 3347.

(27) Hollis, L. S.; Lippard, S. J. *J. Am. Chem. Soc.* **1983**, *105*, 3494.

(28) Barton, J. K.; Szalda, D. J.; Rabinowitz, H. N.; Waszczak, J. V.; Lippard, S. J. *J. Am. Chem. Soc.* **1979**, *101*, 1434.

(29) Faggiani, R.; Lock, C. J. L.; Pollock, R. J.; Rosenberg, B.; Turner, G. *Inorg. Chem.* **1981**, *20*, 804.

(30) Faggiani, R.; Lippert, B.; Lock, C. J. L.; Speranzini, R. A. *J. Am. Chem. Soc.* **1981**, *103*, 111.

(31) Lippert, B.; Neugebauer, D.; Schubert, U. *Inorg. Chim. Acta* **1980**, *46*, L11.

(32) Laurent, J.-P.; Lepage, P.; Dahan, F. *J. Am. Chem. Soc.* **1982**, *104*, 7335.

(33) Hollis, L. S.; Lippard, S. J. *Inorg. Chem.* **1983**, *22*, 2600.

**Table VIII.** Comparative Data for 4:4 and 3:5 Complexes

| compd | M–M, Å | $\lambda_{max}$(abs), nm | $\lambda_{max}$(em), nm | ref |
|---|---|---|---|---|
| 4:4 Structural Type$^a$ | | | | |
| $[Pt_2(\mu\text{-}P_2O_5H_2)_4]^{4-}$ | 2.925 (1) | 368 | 514 | 8, 19 |
| $Ir_2(\mu\text{-}Pz)_2(COD)_2$ | 3.216 (1) | 498 | 687 | 10, 20 |
| $Rh_2(CO)_2Cl_2(\mu\text{-}dpm)_2$ | 3.2386 (5) | 442 | 877 | 21, 22 |
| $Rh_2(CO)_2Cl_2(\mu\text{-}dpa)_2$ | 3.369 (1) | 465 | 699, 900 | 22, 23 |
| $[Rh_2(\mu\text{-}CN(CH_2)_3NC)_4]^{2+}$ | 3.242 (1) | 553 | 656, 830 | 24 |
| $[Rh_2(\mu\text{-}CNCMe_2CH_2CH_2CMe_2NC)_4]^{2+}$ | 3.262 (1) | 526 | 614 | 24 |
| $[Rh_2(CNC_6H_5)_2]^{2+}$ | 3.193 | 568 | 697 | 12 |
| $Rh_2(COD)_2(\mu\text{-}mhp)_2$ | 3.267 (1) | 420 | | 25, 26 |
| $Ir_2(COD)_2(\mu\text{-}mph)_2$ | 3.242 (2) | 484 | 615 | 25, 26 |
| **4** | 3.079 (2) | 470 | 530, 645 | this work |
| $PtCl_2Rh(CO)Cl(\mu\text{-}Ph_2PCH_2AsPh_2)_2$ | 3.043 | | | 14 |
| $[Pt_2(NH_3)_4(\mu\text{-}C_5H_4NO)_2]^{2+}$ht | 2.8981 (5) | | | 27 |
| $[Pt_2(NH_3)_4(\mu\text{-}C_5H_4NO)_2]^{2+}$hh | 2.8767 (7) | | | 27 |
| $[Pt_2(NH_3)_4(\mu\text{-}C_6H_7N_2O_2)_2]^{2+}$ht | 2.974 | | | 28 |
| $[Pt_2(NH_3)_4(\mu\text{-}C_5H_5N_2O_2)_2]^{2+}$ht | 2.954 (2) | | | 29 |
| $[Pt_2(NH_3)_4(\mu\text{-}C_5H_6N_3O)_2]^{2+}$ht | 2.981 (2) | | | 30 |
| $[Pt_2(NH_3)_4(\mu\text{-}C_6H_7N_2O_2)_2]^{2+}$hh | 2.909 (3) | | | 31 |
| $[Pt_2(NH_3)_4(\mu\text{-}C_4H_5N_2O_2)_2]^{2+}$hh | 3.131 | | | 32 |
| $[Pt_2(en)_2(\mu\text{-}C_5H_4NO)_2]^{2+}$hh | 2.992 (1) | | | 33 |
| $[Pt_2(en)_2(\mu\text{-}C_5H_4NS)_2{}^{2+}$hh | 3.083 (1) | | | 34 |
| $[Pt_2Cl_2(\mu\text{-}C_5H_4NSC_2H_4NH_2)_2]^{2+}$ht | 2.956 (1) | | | 34 |
| $[Pd_2(bpy)_2(\mu\text{-}C_6H_7N_2O_2)_2]^{2+}$hh | 2.848 (1) | | | 35 |
| $[Pd_2(en)_2(\mu\text{-}C_5H_4NO)_2]^{2+}$hh | 2.981 (1) | | | 36 |
| $[PtPd(NH_3)_4(\mu\text{-}C_5H_5N_2O_2)_2]^{2+}$hh | 2.927 (1) | | | 37 |
| 5:3 Structural Type | | | | |
| **1** | 2.708 (2) | | | this work |
| **2** | 2.688 (2) | | | this work |
| **3** | 2.703 (2) | | | this work |
| $ClPtRh(CO)Cl_2(\mu\text{-}Ph_2PCH_2AsPh_2)_2$ | 2.692 (1) | | | 14 |
| $IPtRh(CO)Cl_2(\mu\text{-}Ph_2PCH_2AsPh_2)_2$ | 2.737 (3) | | | 14 |
| $ClPdRh(CO)Cl_2(\mu\text{-}Ph_2P_2H_4N)_2$ | 2.594 (1) | | | 13 |
| $[Rh_2(\mu\text{-}(Me_2PCH_2)_2PMe)_2(CO)_2]^{2+}$ | 2.771 (1) | | | 38 |
| $[Rh_2(\mu\text{-}(Me_2PCH_2)_2PMe)_2(CO)I]$ | 2.735 (1) | | | 39 |

[a] hh = head-to-head; ht = head-to-tail.

compilation of data for a group of structurally characterized complexes of this type. These are characterized by metal–metal separations in the range 2.8–3.4 Å and intense absorption bonds that have been assigned to an allowed $\sigma_d^* \rightarrow \sigma_p$ electronic transition. Many of these 4:4 complexes exhibit relatively long-lived photoemissions in solution. The relatively long metal–metal distances, which exceed the range (2.5–2.8 Å) generally associated with single bonds between two metal ions in this region of the periodic table, are consistent with the bonding scheme generally used for these complexes. This focuses on overlap of the filled $d_{z^2}$ and empty $p_z$ orbitals on the two metal centers and accounts for the stability of the M–M bond through second-order effects resulting from mixing of the filled $\sigma_d$ and $\sigma_d^*$ orbitals with the empty $\sigma_p$ and $\sigma_p^*$ levels, which have similar symmetries.[1] Despite the relatively long M–M separations seen within this group, the bonding betwen the two metals is the only factor contributing to the dimerization of unbridged rhodium isocyanide dimers typified by $[Rh_2(CNPh)_8]^{2+}$.[12] The characteristics of **4** are all very typical of complexes of the 4:4 type.

In this context, the structure of **1** is quite remarkable. It is even more remarkable when one realizes that the spectroscopic data for $[Rh_2(CNR)_4(\mu\text{-}dpm)_2]^{2+}$ (R = Me, Bu$^t$)[2,5] and $[Pt_2(CNBu^t)_4(\mu\text{-}dpm)_2]^{4+}$ [40,41] indicate that these have the anticipated 4:4 structures. These observations give a key to an important factor, asymmetry, that governs the stability of the 3:5 arrangement relative to the more symmetrical 4:4 structure. Notice that most of the 4:4 complexes in Table VIII have a symmetrical structure in which the two metal centers and their coordination environments are identical. Complex **4** and $PtCl_2Rh(CO)Cl(\mu\text{-}Ph_2CH_2AsPh_2)_2$ are exceptions. Most of the known complexes with 3:5 structures involve two different metal centers, rhodium and either platinum or palladium, and are, therefore, inherently unsymmetrical in their dimetallic core. The exceptions are $[Rh_2(\mu\text{-}(Me_2PCH_2)_2PMe)_2(CO)_2]^{2+}$ and $[Rh_2(\mu\text{-}(Me_2PCH)_2PMe)_2(CO)I]^+$, which have the bridging triphosphine ligands arranged in an unsymmetrical fashion.[38,39] This involves coordination of all four terminal $PMe_2$ groups to one rhodium, while the two internal PMe groups bind the other rhodium.

Complexes of the 3:5 structural type share the following characteristics. They have metal–metal distances that fall into a relatively narrow range (2.59–2.74 Å) that is significantly shorter than the range for complexes of the 4:4 type. These metal–metal distances are compatible with the presence of single bonds between the two metal centers. Complexes of 3:5 structural type lack the intense proximity shifted features that dominate the absorption spectra of the 4:4 type. From comparison of the spectra of **2** and **3** with **1** it appears that the low-energy absorption of **2** and **3** and the red or orange colors of the other 3:5 complexes in Table IV arise from halide-to-metal charge-transfer transitions along the X–M–M′ axis.

The metal–metal bonding within the 3:5 complexes can be viewed in two ways. If each metal retains the d$^8$ configuration that was present in the components from which these complexes were built, then the metal–metal bond is of the donor/acceptor type. The rhodium center acts as a two electron donor and bonds the platinum center in a donor/acceptor fashion. In this context it is important to note that a number of complexes with

---

(34) Umakoshi, K.; Kinoshita, I.; Fukui-Yasuba, Y.; Matsumoto, K.; Ooi, S.; Nakai, H.; Shiro, M. *J. Chem. Soc., Dalton Trans.* **1989**, 815.

(35) Micklitz, W.; Sheldrick, W. S.; Lippert, B. *Inorg. Chem.* **1990**, *29*, 211.

(36) Matsumoto, K.; Moriyama, H.; Suzuki, K. *Inorg. Chem.* **1990**, *29*, 2096.

(37) Micklitz, W.; Riede, J.; Huber, B.; Müller, G.; Lippert, B. *Inorg. Chem.* **1988**, *27*, 1979.

(38) Balch, A. L.; Olmstead, M. M.; Oram, D. E. *Inorg. Chem.* **1986**, *25*, 298.

(39) Balch, A. L.; Oram, D. E. *J. Organomet. Chem.* **1988**, *349*, 245.

(40) Langrick, C. R.; Pringle, P. G.; Shaw, B. L. *J. Chem. Soc., Dalton Trans.* **1984**, 1233.

(41) Attempts in this laboratory to prepare $[Pt_2(CNMe)_4(\mu\text{-}dpm)_2)]^{4+}$ have only produced the chelated monomer $[Pt(CNMe)_2(dpm)]^{2+}$.

unsupported (unbridged) metal–metal donor/acceptor bonds are known.[42,43] In the present context ($\eta^5$-$C_5H_5$)(CO)$_2$Rh→Pt($C_6F_5$)$_2$(CO) is particularly relevant because of the Rh–Pt bond.[43] The Rh–Pt bond length (2.750 (1) Å) in this complex is just slightly longer than the Rh–Pt bonds in **1**–**3**. Alternately, complexes **1**–**3** can be formulated as species involving a $d^9$ Pt(I) center and a $d^7$ Rh(II) center with a metal–metal bond resulting from paring of two of these d electrons in the normal covalent sense. We favored this latter view in cases such as ClPtRh(CO)$Cl_2$($\mu$-$Ph_2PCH_2AsPh_2$)$_2$[14] and ClPdRh(CO)$Cl_2$($\mu$-$Ph_2PC_6H_4N$)$_2$,[13] where the metal–metal bond formation was accompanied by apparent oxidative addition of a Pt–Cl bond to the rhodium center. In either scheme the platinum center achieves a 16-electron count, while the rhodium center has 18 electrons.

In constructing Table VIII, we have omitted a number of other substances with 4:4 structures. Prominent among these are compounds where a ligand bridge holds two planar $d^8$ complexes within one molecule but does not bring them close enough to interact. Examples include $Ir_2(CO)_2Cl_2(\mu\text{-}Ph_2P(CH_2)_nPPh_2)_2$ ($n$ = 3 and 4), which show electronic absorption spectra similar to that of Ir(CO)Cl($PPh_3$)$_2$ and long Ir–Ir distances.[44,45] We have also excluded substances with short metal–metal separations but with a side-by-side rather than face-to-face arrangement of the two coordination environments. A relevant example is $Rh_2(\mu\text{-}Cl)_2(COD)_2$, which has a planar $Rh_2(\mu\text{-}Cl)_2$ core and a Rh···Rh separation of 3.12 Å.[46] Such side-by-side dimers do not show the interesting metal–metal interactions that are found in face-to-face complexes because the out-of-plane $d_{z^2}$ and $p_z$ orbitals are no longer able to interact in the side-by-side geometry.[3]

Polynuclear species built upon the 4:4 structural motif are known. Thus, $[Rh_3(CNCH_3)_6(\mu\text{-}Ph_2PCH_2P(Ph)CH_2PPh_2)_2]^{3+}$ has a face-to-face structure that can be described as 4:4:4.[47] A corresponding 3:4:5 structure for a trinuclear complexes is an alternative. In the solid-state, complexes like $[Pt_2(NH_3)_2(\mu\text{-}C_5H_4NO)_2]^{2+}$ ($C_5H_4NO$ is $\alpha$-pyridonate) associate through close Pt···Pt contacts to form columnar stacks that can be viewed as a chain of the ···4:4:4:4··· type. Ir(CO)$_3$Cl has a solid-state structure that also appears to be an infinite chain of the ···4:4:4:4··· type, but the Ir–Ir distance (2.844 (1) Å) is shorter than expected.[48] The structure of $[Ir(CNMe)_4{}^+]_n$, which certainly is polymeric,[49,50] could belong to a 4:(4)$_n$:4 or a 5:(4)$_n$:3 pattern. Its novel photodissociation to form monomeric $[Ir(CNMe)_4]^+$ is a characteristic that is somewhat at odds with a 4:(4)$_n$:4 structure.

There is another structural type that is related to the 3:5 complexes. This is the 3:4 structural type, **C**, which is conceptually obtained from **B** by the loss of a ligand trans to the M–M′ bond.[51–54]

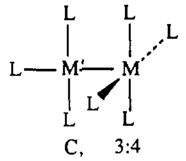

C, 3:4

With two $d^8$ metal centers, complexes of this type possess 16-electron counts at each metal and a donor/acceptor metal–metal bond where M acts as the donor. These complexes typically have M–M′ distances that are characteristic of normal single bonds (i.e. they are similar to what is seen for 3:5 complexes). Representative examples include $[Pt_2Me_3(\mu\text{-}dpm)_2]^+$ (Pt–Pt = 2.769 (1) Å),[51] $Rh_2(1,2\text{-}O_2C_6Cl_4)(CO)(\mu\text{-}dpm)_2$ (Rh–Rh = 2.637 (1) Å),[53] and $[(NH_3)_2Pt(C_5N_6N_3O)_2Pd(NH_3)]^+$ (Pd–Pt = 2.511 (1) Å).[54] Examples of the chemical interconversion of complexes of the 3:5 and 3:4 types are readily foreseen, but none of the complexes examined here shows any detectable tendency to dissociate a ligand from rhodium.

## Experimental Section

**Preparation of Compounds.** $[Pt(dpm)_2]Cl_2$,[55] $Pt(CN)_2(dpm)_2$,[56] $[Pt(CNMe)_4](PF_6)_2$,[57] $[Rh(CNMe)_4](BPh_4)$,[58] and $[Rh(CNBu^t)_4](PF_6)$[56] were prepared by standard routes. Methyl isocyanide was purchased from Quantum Design and vacuum distilled prior to use. *tert*-Butyl isocyanide and dpm were purchased from Aldrich and used without further purification. The new compounds described here are stable to moisture and air and can be prepared without recourse to inert-atmosphere techniques.

**$[(MeNC)PtRh(CNMe)_3(\mu\text{-}dpm)_2](PF_6)_3$ (1). Method A.** Methyl isocyanide (3.9 mg (0.096 mmol)) was added to a stirred solution of 100 mg (0.096 mmol) of $[Pt(dpm)_2]Cl_2$ in 15 mL of acetone. After 5 min, 56.0 mg (0.096 mmol) of $[Rh(CNMe)_4](BPh_4)$ was added. An intense magenta color formed, but the color quickly dissipated upon mixing. The final solution was yellow. After 15 min, 100 mg (0.613 mmol) of ammonium hexafluorophosphate in 10 mL of methanol was added. The solution was allowed to stir, and after 5 min, it was filtered through Celite. The volume was reduced under vacuum. Addition of diethyl ether caused an off-white precipitate to form. The solid was collected by filtration and dried in air. Recrystallization was achieved by dissolution in acetonitrile, filtration, and precipitation with diethyl ether (yield: 85%).

**Method B.** Methyl isocyanide, 3.9 mg (0.095 mmol), was added to a solution of 90 mg (0.095 mmol) of $[Rh(CO)(dpm)_2](PF_6)$ in 10 mL of dichloromethane. The color of initial pale yellow solution intensified, and after 2 min, 62 mg (0.095 mmol) of $[Pt(CNCH_3)_4](PF_6)_2$ was added. A deep magenta color immediately formed and quickly dissipated upon mixing. The resulting pale yellow solution was stirred for 15 min, and then 100 mg (0.613 mmol) of ammonium hexafluorophosphate in 10 mL of methanol was added. The resulting solution was filtered through Celite, and the volume was reduced under vacuum. Addition of ethyl ether forced an off-white crystalline solid to precipitate. The solid was collected by filtration and washed with diethyl ether. Recrystallization was achieved by dissolution in acetonitrile, filtration, and precipitation with diethyl ether (yield: 80%). Infrared: $\nu_{CN}$ = 2230 (s) cm$^{-1}$.

**$[(MeNC)PtRhCl(CNMe)_2(\mu\text{-}dpm)_2](PF_6)_2$ (2).** Methyl isocyanide (11.9 mg (0.29 mmol)) was added to a stirred solution of 100 mg (0.096 mmol) of $[Pt(dpm)_2]Cl_2$ in 15 mL of acetone. After 2 min, 75 min (0.096 mmol) of Rh(CO)Cl($AsPh_3$)$_2$ was added to produce a light orange solution. Addition of 100 mg (0.613 mmol) of ammonium hexafluorophosphate in 15 mL of methanol caused the solution to lighten to yellow. After being stirred for 15 min, the solution was filtered through Celite. Reduction of the solvent volume and addition of diethyl ether resulted in precipitation of a yellow crystalline solid. The product was collected by filtration and washed with diethyl ether and dried in air. Recrystallization was achieved by dissolution in a minimum volume of dichloromethane, filtration, and addition of diethyl ether to precipitate the

---

(42) Einstein, F. W. B.; Jones, T.; Pomeroy, R. K.; Rushman, P. *J. Am. Chem. Soc.* **1984**, *106*, 2707. Davis, H. B.; Einstein, F. W. B.; Glavina, P. G.; Jones, T.; Pomeroy, R. K.; Rushman, P. *Organometallics* **1989**, *8*, 1030. Batchelor, R. J.; Davis, H. B.; Einstein, F. W. B.; Pomeroy, R. K. *J. Am. Chem. Soc.* **1990**, *112*, 2036.

(43) Usón, R.; Forniés, J.; Espinet, P.; Fortuño, C.; Tomas, M.; Welch, A. J. *J. Chem. Soc., Dalton Trans.* **1988**, 3005.

(44) Wang, H.-H.; Pignolet, L. H.; Reedy, P. E., Jr.; Olmstead, M. M.; Balch, A. L. *Inorg. Chem.* **1987**, *26*, 377.

(45) Balch, A. L.; Davis, B. J.; Olmstead, M. M. *Inorg. Chem.* **1990**, *29*, 3066.

(46) Dahl, L. F.; Martell, C.; Wampler, D. L. *J. Am. Chem. Soc.* **1961**, *83*, 1761.

(47) Balch, A. L.; Fossett, L. A.; Nagle, J. K.; Olmstead, M. M. *J. Am. Chem. Soc.* **1988**, *110*, 6732.

(48) Reis, A. H., Jr.; Hagley, V. S.; Peterson, S. W. *J. Am. Chem. Soc.* **1977**, *99*, 4184.

(49) Geoffroy, G. L.; Bradley, M. G.; Keeney, M. E. *Inorg. Chem.* **1978**, *17*, 777.

(50) Carr, N.; Crossley, J. G.; Dent, A. J.; Gouge, J. R.; Greaves, G. N.; Jarrett, P. S.; Orpen, A. G. *J. Chem. Soc., Chem. Commun.* **1990**, 1369.

(51) Brown, M. P.; Cooper, S. J.; Frew, A. A.; Manojlovic-Muir, Lj.; Muir, K. W.; Puddephatt, R. J.; Seddon, K. R.; Thomson, M. A. *Inorg. Chem.* **1981**, *20*, 1500.

(52) Haines, R. J.; Meintjies, E.; Laing, M. *Inorg. Chim. Acta* **1979**, *36*, L403.

(53) Ladd, J. A.; Olmstead, M. M.; Balch, A. L. *Inorg. Chem.* **1984**, *23*, 2318.

(54) Krumm, M.; Lippert, B.; Randaccio, L.; Zangrando, E. *J. Am. Chem. Soc.* **1991**, *113*, 5129.

(55) Pringle, P. G.; Shaw, B. L. *J. Chem. Soc., Chem. Commun.* **1982**, 956.

(56) Hassan, F. S. M.; Markhan, D. P.; Pringle, P. G.; Shaw, B. L. *J. Chem. Soc., Dalton Trans* **1985**, 279.

(57) Miller, J. S.; Balch, A. L. *Inorg. Chem.* **1972**, *11*, 2069.

(58) Balch, A. L.; Miller, J. *J. Organomet. Chem.* **1971**, *32*, 263.

**Table IX.** Crystal Data and Data Collection and Structure Solution Parameters for **1**–**4**

| | 1 | 2 | 3 | 4 |
|---|---|---|---|---|
| formula | $C_{60.92}H_{62.22}F_{18}N_{4.54}O_{0.46}P_7PtRh$ | $C_{57}H_{54.5}ClF_{12}N_{3.5}P_6PtRh$ | $C_{58}H_{53}IF_{12}N_4P_6PtRh$ | $C_{64.5}H_{64}F_6N_4OP_5PtRh$ |
| fw | 1722.1 | 1535.8 | 1644.8 | 1478 |
| color and habit | ivory pyramids | gold prisms | yellow prisms | red needles |
| cryst system | monoclinic | triclinic | triclinic | orthorhombic |
| space group | $P2_1/n$ (No. 14) | $P\bar{1}$ (No. 2) | $P\bar{1}$ (No. 2) | $Pnma$ (No. 62) |
| $a$, Å | 15.724 (6) | 11.465 (4) | 11.531 (5) | 35.723 (11) |
| $b$, Å | 18.157 (5) | 14.832 (6) | 14.682 (6) | 15.214 (7) |
| $c$, Å | 25.13 (2) | 19.712 (10) | 19.849 (14) | 12.542 (5) |
| $\alpha$, deg | | 87.71 (4) | 86.210 (5) | |
| $\beta$, deg | 97.52 (5) | 79.43 (4) | 78.260 (5) | |
| $\gamma$, deg | | 67.98 (3) | 68.77 (3) | |
| $V$, Å$^3$ | 7112 (6) | 3056 (2) | 3067 (3) | 6816 (5) |
| $T$, K | 130 | 130 | 130 | 130 |
| $Z$ | 4 | 2 | 2 | 4 |
| $d_{calcd}$, g mm$^{-3}$ | 1.608 | 1.669 | 1.781 | 1.440 |
| $\mu$(Mo K$\alpha$), mm$^{-1}$ | 2.443 | 2.849 | 3.295 | 2.481 |
| range of transm factors | 0.32–0.60 | 0.43–0.70 | 0.09–0.70 | 0.17–0.85 |
| $R(F_o)^a$ | 0.073 | 0.041 | 0.042 | 0.065 |
| $R_w(F_o)^a$ | 0.076 | 0.042 | 0.044 | 0.065 |

$^a$ $R = \sum\|F_o| - |F_c\|/\sum|F_o|$; $R_w = \sum\|F_o| - |F_c\|w^{1/2}/\sum|F_o|w^{1/2}$.

product (yield: 69%). Infrared: $\nu_{CN}$ = 2218 (s) cm$^{-1}$. Some preparations of this complex contain absorption bands at 444 and 400 nm which result from an impurity that can be removed by careful recrystallization.

**$[(MeNC)PtRhI(CNMe)_2(\mu\text{-dpm})_2](PF_6)_2$ (3).** To an acetone solution (10 mL) of 100 mg (0.06 mmol) of **1** was added 15.4 mg (0.06 mmol) of $I_2$. A yellow color slowly formed, and after the mixture was stirred for 15 min, 100 mg (0.613 mmol) of ammonium hexafluorophosphate in 10 mL of methanol was added. After being stirred for 5 min, the solution was filtered though Celite. The volume was reduced under vacuum, and addition of diethyl ether produced a yellow precipitate. The product was collected by filtration and washed with diethyl ether. The solid was recrystallized by dissolution in a minimum volume of acetonitrile, filtration, and precipitation with ethyl ether (yield: 80%). Infrared: $\nu_{CN}$ = 2212 (s) cm$^{-1}$.

**$[(NC)_2PtRh(CNBu^t)_2(\mu\text{-dpm})_2](PF_6)$ (4).** To the colorless solution formed by dissolving 94 mg (0.092 mmol) of $Pt(CN)_2(dpm)_2$ in 10 mL of dichloromethane was added 54 mg (0.092 mmol) of $[Rh(CNBu^t)_4](PF_6)$. A deep orange color rapidly appeared, and after 10 min of stirring, a solution of 100 mg (0.61 mmol) ammonium hexafluorophosphate in 10 mL of methanol was added. The solution was filtered through Celite. Reduction of solvent volume and addition of diethyl ether yielded a crystalline orange solid. The solid was collected by filtration and dried in air. Recrystallization was achieved by dissolution by a minimal volume of dichloromethane, filtration, and addition of ethyl ether to precipitate the product from the filtrate (yield: 81%).

**Physical Measurements.** The $^{31}P\{^1H\}$ NMR spectra were recorded on a General Electric QE-300 NMR spectrometer that operates at 121.7 MHz with an external 85% phosphoric acid standard and the high-field positive convention for reported chemical shifts. Infrared measurements were recorded on an IBM IR32 spectrometer. Electronic spectra were recorded with a Hewlett-Packard 8450A diode array spectrometer. Uncorrected emission spectra were obtained through the use of a Perkin-Elmer MPF-44B fluorescence spectrometer.

**X-ray Data Collection. $[(MeNC)PtRh(CNMe)_3(\mu\text{-dpm})_2](PF_6)_3\cdot 0.46(C_2H_5)_2O\cdot 0.54CH_3CN$ (1).** Ivory crystals were obtained by slow diffusion of ethyl ether into an acetonitrile solution of the complex A single crystal was mounted on a glass fiber with silicon grease and placed into the 130 K nitrogen stream of a Siemens R3m/v diffractometer with a modified Enraf-Nonius low-temperature apparatus. Unit cell parameters were determined by least-squares refinement of 29 reflections with 6.3° < $2\theta$ < 30.1°. The axial lengths and monoclinic crystal system were verified by examination of axial photos. The two check reflections showed only random fluctuations (<3%) in intensity throughout the data collection. The data were corrected for Lorentz and polarization effects. Crystal data are given in Table IX.

**$[(MeNC)PtRhCl(CNMe)_2(\mu\text{-dpm})_2](PF_6)_2\cdot 0.5CH_3CN$ (2).** Yellow crystals were grown by slow diffusion of diethyl ether into an acetonitrile solution of the complex. The crystal was handled and mounted as described above. Unit cell parameters were determined by least-squares refinement of 28 reflections with 17.2° < $2\theta$ < 30.5°. The axial lengths and triclinic crystal system were verified by examination of axial photos. The two check reflections showed only random fluctuations (<2%) in intensity throughout the data collection. The data were corrected for Lorentz and polarization effects.

**$[(MeNC)PtRhI(CNMe)_2(\mu\text{-dpm})_2](PF_6)_2\cdot CH_3CN$ (3).** Yellow crystals were grown by slow diffusion of diethyl ether into an acetonitrile solution of the complex. The crystal was handled and mounted as described above except a Syntex P2$_1$ diffractometer equipped with a modified LT-1 low-temperature apparatus was used. Unit cell parameters were determined by least-squares refinement of 14 reflections with 13.8° < $2\theta$ < 30.9°. The axial lengths were verified by examination of axial photos. The two check reflections showed only random fluctuations (<2%) in intensity throughout the data collection. The data were corrected for Lorentz and polarization effects.

**$[(NC)_2PtRh(CNBu^t)_2(\mu\text{-dpm})_2](PF_6)\cdot 0.5(C_2H_5)_2O\cdot 0.5MeOH$ (4).** Orange crystals were obtained by slow diffusion of diethyl ether through a 2-mm layer of MeOH into a dichloromethane solution of the complex. The crystals were handled as in **1**. Unit cell parameters were determined by least-squares refinement of 12 reflections with 8.0° < $2\theta$ < 18.3°. The axial lengths and orthorhombic crystal system were verified by examination of axial photos. The two check reflections showed only random fluctuations (<2%) in intensity throughout the data collection. The data were corrected for Lorentz and polarization effects.

**Solution and Structure Refinement. $[(MeNC)PtRh(CNMe)_3(\mu\text{-dpm})_2](PF_6)_3\cdot 0.46(C_2H_5)_2O\cdot 0.54CH_3CN$ (1).** Calculations were performed on a Microvax computer with SHELXTL PLUS 4.11 software. Scattering factors and corrections for anomalous dispersion were taken from a standard source.[59] Successful solution and refinement of the structure were achieved in the centrosymmetric space group $P2_1/n$ (No. 14). The positions of the platinum and rhodium atoms were determined from a Patterson map. Both metals, all phosphorus atoms, N(1)–N(4), and F(1)–F(6) were refined with anisotropic thermal parameters, while all other atoms were refined with isotropic thermal parameters. Hydrogen atoms were fixed to all carbon atoms where chemically justified. The hydrogen atom positions were calculated using a riding model with C–H vector fixed at 0.96 Å and a thermal parameter 1.2 times that of the host carbon. Two of the hexafluorophosphate anions are disordered. The largest peak in the final difference map is equivalent to 1.76 e/Å$^3$. An absorption correction was applied.[60]

**$[(MeNC)PtRhCl(CNMe)(\mu\text{-dpm})_2](PF_6)_2\cdot 0.5CH_3CN$ (2).** The structure was solved by Patterson methods in the triclinic space group $P\bar{1}$ (No. 2). Refinement followed procedures outlined above. Final refinement was carried out with anisotropic thermal parameters for all non-carbon atoms excluding the half-occupancy acetonitrile and including C(3)–C(6). All other atoms were refined with isotropic thermal parameters. Hydrogen atoms were treated as described above, and an absorption correction was applied.[60] The largest peak in the final difference map is equivalent to 1.31 e/Å$^3$ and is 0.656 Å from C(57). The largest shift/esd in the final cycle of refinement was -0.001 for the overall scale.

---

(59) *International Tables for X-ray Crystallography.* Kynoch Press: Birmingham, England, 1974; Vol. 4.

(60) The method obtains an empircal absorption tensor from an expression relating $F_o$ and $F_c$: Moezzi, B. Ph.D. Thesis, University of California, Davis, 1987.

**$[(MeNC)PtRhI(CNMe)_2(\mu\text{-dpm})_2](PF_6)_2\cdot CH_3CN$ (3).** The structure was solved by direct methods in the triclinic space group $P\bar{1}$ (No. 2). Refinement procedures were employed as described above. All Pt, Rh, I, P, and F atoms were refined with anisotropic thermal parameters, while all others were refined with isotropic thermal parameters. Hydrogen atoms were included as outlined above. The largest peak in the final difference map is equivalent to 0.84 e/Å$^3$ and is 0.747 Å from C(57). The largest shift/esd in the final cycle of refinement was 0.002 for $U11$ of C(31).

**$[(NC)_2PtRh(CNBu^t)_2(\mu\text{-dpm})_2](PF_6)\cdot 0.5(C_2H_5)_2O\cdot 0.5MeOH$ (4).** The structure was solved by Patterson methods in the orthorhombic space group *Pnma* (No. 62). Refinement procedures were as described above. All atoms except carbon and hydrogen and excluding solvent were refined with anisotropic thermal parameters, while all others were refined with isotropic thermal parameters. Hydrogen atoms were included as outlined above. The largest peak in the final difference map is equivalent to 1.55 e/Å$^3$ and is 0.928 Å from C(36). An absorption correction was applied.

**Acknowledgment.** We thank the National Science Foundation (Grants CHE 894209 and CHE 9022909) for support, Johnson Matthey Inc. for a loan of platinum and rhodium salts, and Dr. M. M. Olmstead and B. C. Noll for assistance with the X-ray crystallography. V.J.C. thanks the International Precious Metals Institute for a fellowship.

**Supplementary Material Available:** Tables of atomic coordinates, bond distances, bond angles, anisotropic thermal parameters, hydrogen atom positions, and crystal data for **1**–**4** (33 pages). Ordering information is given on any current masthead page.